J Mammal Evol (2018) 25:197–211
DOI 10.1007/s10914-016-9372-7

ORIGINAL PAPER

Functional Anatomy of the Forelimb of *Plesiotypotherium achirense* (Mammalia, Notoungulata, Mesotheriidae) and Evolutionary Insights at the Family Level

Marcos Fernández-Monescillo[1] · **Bernardino Mamani Quispe**[2] · **François Pujos**[1] · **Pierre-Olivier Antoine**[3]

Published online: 9 January 2017

Abstract In the present work, we provide muscular reconstruction and we infer functional properties of the forelimb of *Plesiotypotherium achirense*, a fossil mesotheriid notoungulate from the late Miocene of Achiri (Bolivia). This locality has yielded the widest sample ever available for the forelimb of a mesotheriid. In addition, we propose a qualitative comparison of the forelimb (osteology and myology) at the family level, including the Miocene–Pleistocene mesotheriines *Mesotherium cristatum*, *Plesiotypotherium achirense*, *Caraguatypotherium munozi*, *Plesiotypotherium casirense*, and *Pseudotypotherium* sp, and the late Oligocene trachytheriine *Trachytherus alloxus*. Functional properties are consistent with a digging ability and a "scratch-digger" lifestyle for Mesotheriidae. In general, there are only slight differences among the comparison sample, except for *Mesotherium cristatum,* which reflect significant osteological modifications, likely to help increasing the moment arm while scratch-digging. These features are mainly observable on scapulae (distal border caudally displaced) and humeri (deltoid crest distally oriented and crista supracondylaris lateralis laterally projected).

Keywords South America · Bolivian Altiplano · Late Miocene · Paleomammalogy · Myology

Electronic supplementary material The online version of this article (doi:10.1007/s10914-016-9372-7) contains supplementary material, which is available to authorized users.

✉ Marcos Fernández-Monescillo
mfernandez@mendoza-conicet.gob.ar

[1] Instituto Argentino de Nivología, Glaciología y Ciencias Ambientales (IANIGLA), CCT–CONICET–Mendoza, Avda. Ruiz Leal s/n, Parque Gral, San Martín 5500, Mendoza, Argentina

[2] Departamento de Paleontología, Museo Nacional de Historia Natural, Calle 26 s/n, Cota Cota, La Paz, Estado Plurinacional de Bolivia

[3] Institut des Sciences de l'Evolution, cc64, Université de Montpellier, CNRS, IRD, EPHE, F-34095 Montpellier, France

Introduction

Mesotheriidae is a family of South American native ungulates, assigned to the extinct order Notoungulata. Mesotheriidae includes Trachytheriinae, Oligocene in age, paraphyletic, and mostly represented by *Trachytherus* Ameghino, 1889 (see Billet et al. 2008), and Mesotheriinae, documented from the early Miocene (Colhuehuapian South American Land Mammal Age [SALMA]; Paz et al. 2011) to the late early Pleistocene (Ensenadan SALMA; e.g., *Mesotherium cristatum* Serres, 1867).

Croft (2007) considered that mesotheriines differ from other notoungulates in possessing: (i) hypselodont teeth, (ii) a large diastema between incisors and cheek teeth, and (iii) characteristic trilobed upper molars. Shockey et al. (2007) provided a short history of the group. Representatives of this family have been successively considered as transitional forms between rodents and "pachyderms" (Serres 1867), as rodents (Gervais 1867, 1869), and as prosimian primates (Ameghino 1891, 1906) before their ordinal affinities were set among Notoungulata. Accordingly, the hypothesized lifestyle of these taxa has always been disputed, ranging from aquatic (Serres 1867), running-hopping (Loomis 1914), "scratch digging" (Sydow 1988) sensu Hildebrand (1974, 1985), or cursorial and semiaquatic (Bond et al. 1995). The most recent studies interpreted a scratch-digging way of life and a highly conservative

postcranial skeleton for Mesotheriidae as a whole (Shockey et al. 2007; Shockey and Anaya 2008). According to these authors, Mesotheriidae were probably semifossorial animals that could dig in pursuit of food and/or for building dens.

The paleontological site of Achiri is located in the Pacajes Province of La Paz Department, Bolivia (Fig. 1). This fauna comes from the Mauri Formation (Unit IV), with a late Miocene age constrained by $^{40}Ar/^{39}Ar$ dating for the underlying Ulloma Formation (10.35±06 Ma; Marshall 1992). The Achiri site was first reported in the 1970s (Villarroel 1974; Saint-André 1993), and then excavated by distinct international teams (e.g., IFEA-GEOBOL missions during the 1990s; Saint-André 1993). Our working group, encompassing Bolivian, Argentinian, Spanish, and French paleontologists and geologists, has worked at Achiri during the period 2011–2015. Four decades of fieldwork have resulted in an unparalleled sample of craniomandibular and postcranial material referable to mesotheriids in Achiri, especially for the forelimb, and deposited in several scientific institutions (e.g., MNHN-Bol and MNHN). In Achiri, Mesotheriidae are documented by *Plesiotypotherium achirense* Villarroel, 1974, and *Plesiotypotherium majus* Villarroel, 1974, the former species being widely dominant over the latter in terms of referred specimen abundance.

Qualitative comparisons of the mesotheriid appendicular skeleton were already undertaken by several authors beginning in the last century (Cattoi 1943; Villarroel 1974; Croft et al. 2004; Flynn et al. 2005; Shockey et al. 2007; Cerdeño et al. 2012), but to our knowledge, no work has focused on soft tissue and morphological reconstruction for any mesotheriine thus far. Nevertheless, the comparative studies by Cattoi (1943) and Shockey et al. (2007) have included some muscular indications on postcranial elements, both qualitative and quantitative in the latter reference.

This work aims at (i) reconstructing the osteological and muscular forelimb configuration and inferring the locomotor abilities of the notoungulate *Plesiotypotherium achirense*, according to an unparalleled forelimb sample recovered from Achiri, and (ii) assessing the forelimb osteological changes at the mesotheriid level and discussing how the inferred morpho-functional properties have evolved for the different taxa analyzed.

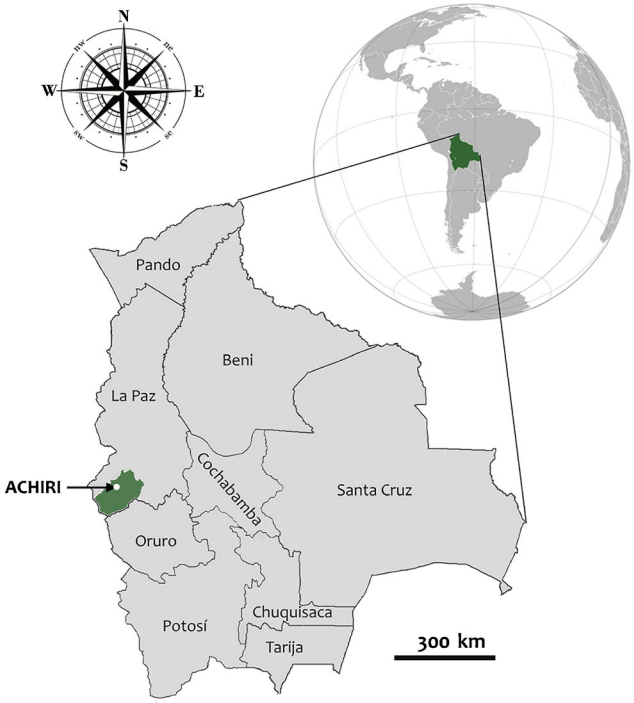

Fig. 1 Location map of the late Miocene fossil-yielding Achiri locality, Pacajes Province, La Paz Department, Bolivia

Material and Methods

Institutional Abbreviations

FLMNH, Florida Museum of Natural History (with UF indicating FLMNHN specimens), Gainesville, USA; GEOBOL, (former) Servicio Geológico de Bolivia, La Paz, Bolivia; IFEA, Institut Français d'Etudes Andines, La Paz, Bolivia; MACN, Museo Argentino de Ciencias Naturales "Bernardino Rivadavia," Buenos Aires, Argentina; MNHN, Muséum national d'histoire naturelle, Paris, France (specimens referred to as PAM or SAL in the text, respectively); MNHN-Bol, Museo Nacional de Historia Natural de Bolivia, La Paz, Bolivia; SGO, Museo Nacional de Historia Natural, Santiago, Chile.

Specimens from Achiri

Plesiotypotherium achirense is the type species of *Plesiotypotherium* (abbreviated below as *Pl.*). The holotype originates from 3-4 km to the west of Achiri village in the place known as Cerro Balcunani (Villarroel 1974). In this study we include also the fossils of *Pl. achirense* recovered from other sites located in the same area: Hanko Hakke, Jakka Pukara, Cerro Pisakeri, and Virgen Pata (see Saint-André 1993). The type material of *Pl. achirense* was described by Villarroel (1974); we added to the original descriptions the unpublished fossils housed in the MNHN and in the MNHN-Bol. The forelimb fossil material is the most abundant known for any mesotheriid (see material list in Online Resource 1).

Plesiotypotherium majus also originates from the Achiri area, with a hypodigm collected between Pirapi Grande and Pirapi Chico southeast to Achiri (Villarroel 1974). We were not able to make any comparison with *Pl. majus*, because it is

documented only by craniomandibular and hind limb remains. To our knowledge, no forelimb specimen has been assigned to this taxon, either originating from early field campaigns or from our own fieldwork.

Comparison Material (Other Mesotheriidae)

We compared with other mesotheriids in order to scrutinize evolutionary changes of the forelimb osteological features, and to infer their functional anatomical evolution at the family level. We include in the comparison the trachytheriine *Trachytherus alloxus* Billet et al. 2008, from the late Oligocene of Salla, Bolivia (Billet et al. 2008). Mesotheriines included within the present study are: *Mesotherium cristatum* from the Pleistocene (Ensenadan) of Paraná basin and La Plata River, Argentina; *Pseudotypotherium* sp. from the Pliocene (Montehermosan) of Monte Hermoso Formation, Buenos Aires Province, Argentina (Rovereto 1914; Cattoi 1943); *Caraguatypotherium munozi* Flynn et al., 2005, from the middle Miocene (pre-Huayquerian and post-Friasian) of Lower Huaylas Formation, Caragua, northern Chile (Flynn et al. 2005); and *Plesiotypotherium casirense* Cerdeño et al., 2012, from the late Miocene of Casira, Potosí Department, Bolivia.

Measurements and Indices

The measurement abbreviations are indicated in Online Resource 2. The measurements were taken with a digital caliper of 150 mm. Quantitative data were analyzed using the software package PAST, version 3.11 (Hammer et al. 2001). The summary of the measurements appear in the Online Resource 3. Biological indices have been used often in biological and paleontological studies in order to infer locomotor abilities (e.g., Maynard Smith and Savage 1956; Elissamburu and Vizcaino 2004; Shockey et al. 2007; Croft and Anderson 2008). The biological indices, derived from the ones used for the forelimb in Croft and Anderson (2008), are indicated in Table 1 and the biological index values are in Table 2.

Anatomical Description

The anatomical descriptions follow the terminology of Schaller (2007) using primarily the terms of the Nomina Anatomica Veterinaria (Waibl et al. 2005), and De Iuliis and Pulerà. (2010) as illustrated in Figs. 2 and 3. We use the following anatomical terms of direction: medial, lateral, cranial (dorsal in the manus), caudal (plantar in the manus), proximal, and distal. We made comparison with extant animals of similar osteological structures with well-known myology and functional anatomical abilities (Taylor 1978; McEvoy 1982; Ebensperger and Bozinovic 2000; Candela and Picasso 2008; Ercoli et al. 2014). In addition, we have compared with extant animals of different locomotor lifestyles including cursorial (Gregory 1912), natatorial (Polly 2007), or scansorial (Cartmill 1974).

All data generated or analyzed during this study are included in this published article [and its supplementary information files].

Description of Forelimb Osteology and Myology

Scapula

The scapular body is rectangular. The main muscles (m.) involved in the fixation of the glenohumeral joint are the m. supraspinatus, m. infraspinatus, and m. subscapularis (Fig. 4; Davis 1949). In addition, there is evidence of a preserved clavicle in both *Pl. achirense* (MNHN ACH 26, 34) and the derived species *Mesotherium cristatum* (MNHN PAM 2) among mesotheriids. In lateral view (Fig. 2a,c), a marked spine runs along the transverse axis bifurcating cranially into a slender acromion (processus hamatus) and caudally into a broad metacromion (processus suprahamatus). The acromion coincides with the origin for the pars acromialis of the m. deltoideus and the metacromion with the omotransversarius (Larson 1993; Muizon 1998; Argot 2001). Proximally in the spine is attached the pars scapularis, and distally the m. trapezius (Fig. 4). The fossa infraspinata is slightly covered by the border of the spine

Table 1 Biological indices used in this study

Name	Abbr.	Formule	Source
Brachial index (radius)	BI(r)	BI(r)=RL/HL*100	Sargis 2002
Humerus robustness index	HRI	HRI=HMW/HL*100	Elissamburu and Vizcaíno 2004
Index of fossorial ability	IFA	IFA=LO/LFU*100	Hildebrand 1985
Ulna robustness index	URI	URI=UMW/LFU*100	Elissamburu and Vizcaíno 2004
Epicondyle index	EI	EI=HDEW/HL*100	Hildebrand 1985
Brachial index (ulna)	BI(u)	BI(u)=UL/HL*100	Croft and Anderson 2008
Radius robustness index	RRI	RRI=RMW/RL*100	This study

Table 2 Biological indices for forelimb bones of the mesotheriid notoungulates analyzed in the current work

Species	Specimen number	BI(r)	HRI	IFA	URI	EI	BI(u)	RRI
Caraguatypotherium munozi	SGO PV 22500 (L)	–	–	**30.64**	**7.72**	–	–	**7.61**
Plesiotypotherium	MNHN ACH 18 (R)	92.56	12.26	–	–	32.27	–	7.81
achirense	MNHN-Bol-V 12687 (R)	89.50	10.50	32.91	9.17	32.27	120.76	6.72
	MNHN-Bol-V 12768 (R)	–	12.87	–	–	31.32	–	–
	MNHN-Bol-V 12768 (L)	–	12.24	–	–	33.33	–	–
	MNHN-Bol-V 12760 (R)	–	–	–	–	–	–	7.39
	Mean value	**91.74**	**11.97**	**32.91**	**9.17**	**32.30**	**120.76**	**7.31**
Plesiotypotherium	MNHN-Bol-V 3724 (R)	93.16	13.84	32.00	8.64	37.55	–	8.49
casirense	MNHN-Bol-V 3724 (L)	–	–	29.57	8.73	–	119.34	8.05
	Mean value	**93.16**	**14.84**	**30.78**	**8.69**	**37.55**	**119.34**	**8.27**
Mesotherium cristatum	PAM 2 (R)	**88.78**	**11.37**	**34.53**	**8.20**	**33.77**	**119.56**	**7.49**
Trachytherus alloxus	MNHN SAL 7 (L)	–	19.09	–	–	32.85	–	–
	MNHN SAL 1738 (L)	–	–	–	8.32	–	–	–
	UF 91933 (L)	90.27	–	–	–	–	–	–
	Mean value	**90.27**	**19.09**	**–**	**8.32**	**32.85**	**–**	**–**

See Table 1 for index abbreviations. R, right; L, left. Mean values are in bold

cranially and by the caudal scapula; both lean over the fossa. The fossa supraspinata is rectangular and relatively larger than the fossa infraspinata, which is triangular in shape (Cattoi 1943). Accordingly, the supraspinatus muscle was probably more developed than the m. infraspinatus. The nutrient canal is located proximally in the fossa infraspinata, and below the suprahamatus process (metacromion) (Fig. 2c). In proximal view (Fig. 2b), the pear-like cavitas glenoidale is laterally convex and slightly medially convex. The lateral side is variable, from convex (MNHN ACH 34), straight (MNHN-Bol-V 8407), to concave (MNHN-Bol-V 12659 and 11690). The proximal cranial border is acute and ends in the supraglenoid tuberosity (tuberculum supraglenoidale), slightly ventrally projected. In this tuberosity inserts the m. biceps brachii. Craniomedially is the strongly developed and mediocranially oriented coracoid process, where the m. coracobrachialis is attached. In caudal view, the m. teres minor is inserted in a marked triangular facet on the tuberculum infraglenoidale of the scapular neck. Likewise, the caput longum of the m. triceps brachii inserts longitudinally in the caudal border of the scapula. In medial view, two surfaces inflated caudally and

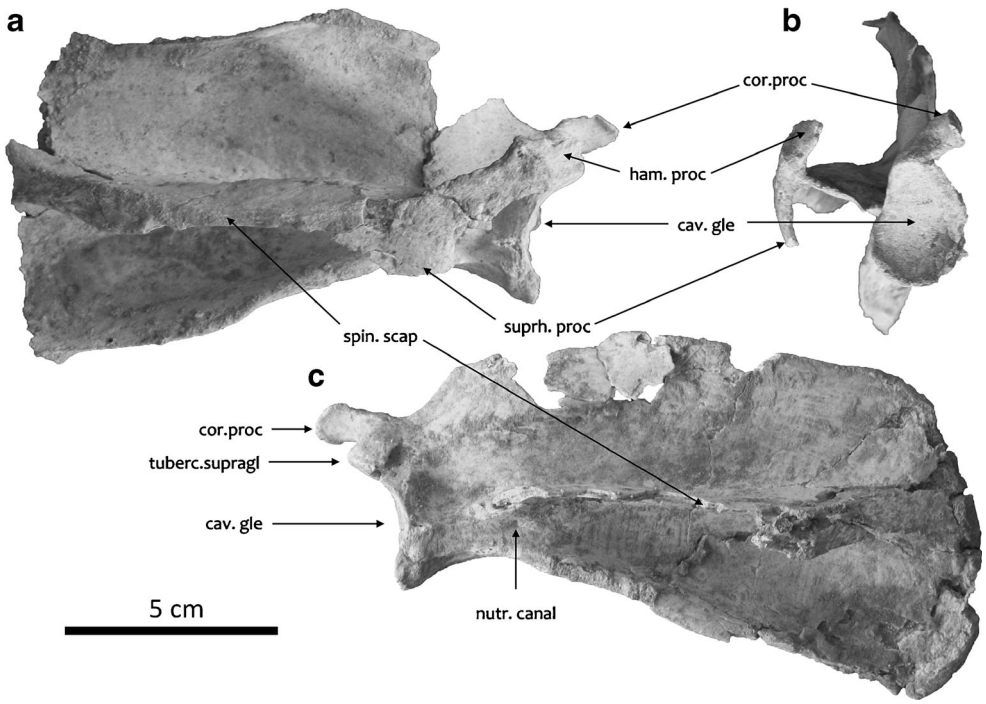

Fig. 2 Scapulae of *Plesiotypotherium achirense*. **a**-**b**, Right scapula MNHN-Bol-V 12617 in lateral and proximal views respectively; **c**, Left scapula MNHN-Bol-V 12617 in lateral view. Abbreviations: *cav.gle*, cavitas glenoidale; *cor. proc*, coracoid process; *ham. proc*, hamatus process (acromion); *nutr. canal*, nutrient canal; *suprh. proc*, suprahamatus process (metacromion); *spin. scap*, spina scapulae; *tuberc. supragl*, tuberculum supraglenoidale

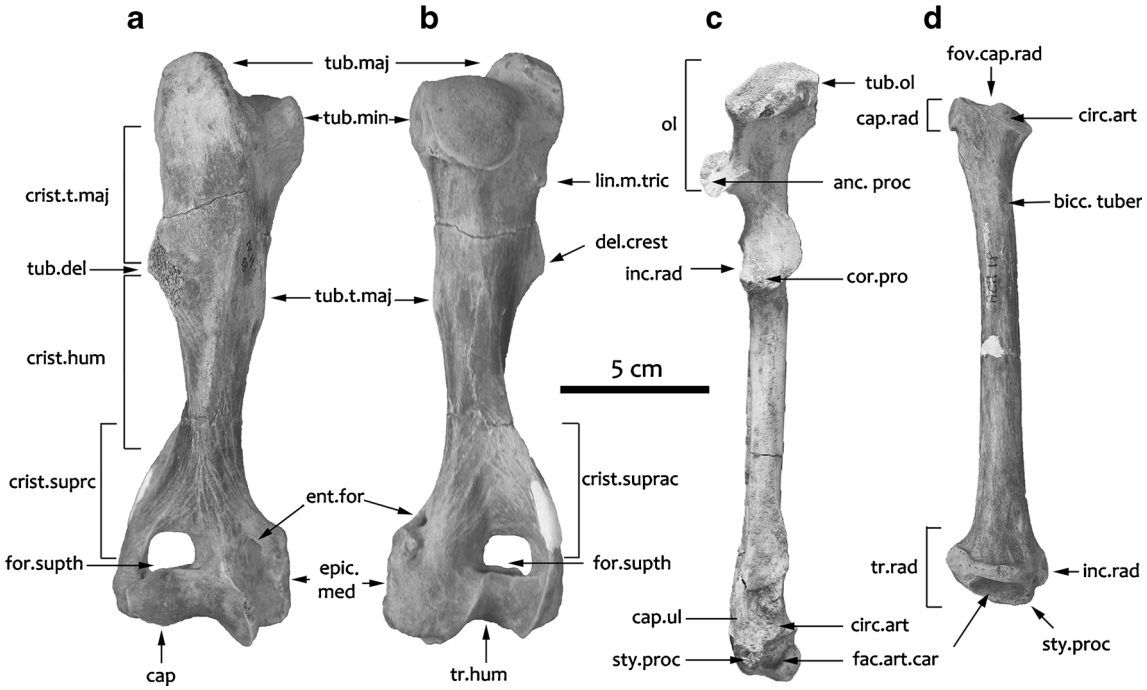

Fig. 3 Anatomical features of the humerus, ulna and radius of *Plesiotypotherium achirense*. **a**-**b**, Right humerus (paratype, MNHN ACH 18) in cranial and distal views, respectively; **c**, Right ulna (MNHN-Bol-V 12687) in cranial view; **d**, Left radius (paratype, MNHN ACH 18) in caudal view. Abbreviations: *anc. proc*, anconeus process; *bicc. tuber*, biccipital tuberosity; *cap.rad*, caput radii; *cap.ul*, caput ulnae; *cap*, capitulum; *circ.art,* circumferentia articularis of the radius; *circ.art*, circumferentia articularis of the ulna; *cor. pro*, coronoid process (processus coronoideus mediallis); *crist.hum*, crista humeri; *crist.suprac*, crista supracondylaris lateralis (epicondylar crest); *crist.t.maj*, crista tubercularis majoris; *ent.for*, entepicondylar foramen; *epic.med*, epicondylus medius (entepicondyle); *fac.art.car*, facies articularis carpea; *for.supth*, foramen supratrochlear; *fov.cap.rad*, fovea capitis radii (radial notch); *inc.rad*, incisura radialis; *inc.rad*, incisura ulnaris; *lin.m.tric*, linea m. tricipitis; *ol*, olecranon; *sty.proc*, styloid process; *tr.hum*, trochlea humeri; *tr.rad*, trochlea radii; *tub.del*, tuberositas deltoidea; *tub.maj*, tuberculum majus; *tub.min*, tuberculum minor; *tub.ol*, tuber olecrani (proximal tubercle); *tub.t.maj*, tuberositas teres major

cranially to the fossa subscapularis coincide with the insertion of the m. subscapularis (Fig. 4).

Humerus

In cranial view (Fig. 5h), salient features are the massive deltopectoral crest (tuberositas deltoidea), the greater tubercle (tuberculum majus), and the proximodistally elongated medial epicondyle or entepicondyle (epicondylus medialis). The well-developed deltopectoral crest hosts the insertion for both the m. deltoideus and the m. pectoralis (Shockey et al. 2007). In lateral, and medial view (Fig. 5c), the humerus has a sigmoid shaft with a constant diaphyseal width. The distal epiphysis is slightly laterally oriented in comparison to the proximal epiphysis because of the torsion of the diaphysis (Cattoi 1943). Proximally, the greater tubercle is highly projected over the humerus head. A deep and triangular facet is located cranial to both tubercles, for the insertion of the m. coracobrachialis (Cattoi 1943). The greater tubercle presents laterally a rounded and deep facet for the m. infraspinatus. Another rounded facet is located distal to this structure. It is delimited by the linea m. tricipitis, which marks the insertion of the pars caput laterale of the tricipitis brachii muscle. In lateral view (Fig. 5a), the greater tubercle is proximally projected. The pars acromialis and pars scapularis of the m. deltoideus attach into the deltoid crest. A wide insertion for both the m. triceps brachii caput accesorium and caput laterale is located distally in the medial humeral neck. In medial view (Figs. 4 and 5c), the large insertion for the m. supraspinatus is situated medial to the tuberculus majus. Lateral to the lesser tubercle inserts the m. subscapularis. Distal to it is the longitudinal and narrow tuberositas teres major in which the m. teres major and m. latissimus dorsi insert. Caudal to them and distal to the neck attaches the medial branch of the m. triceps brachii. In proximal view, cranial to the caput humeri and between the greater and the lesser tuberosity, is the caudally concave intertubercular groove (sulcus intertubercularis). In cranial view (Fig. 5h) the deltopectoral crest is well developed. All these structures determine a wide, laterally oriented deltopectoral plateau. The well-developed crista supracondylaris lateralis receives the m. supinator longus (supinatory muscle brachioradialis), the m. extensor carpi radialis, and m. extensor digitorum communis. Whereas the surface for the origin of the m. extensor carpi ulnaris is located distally, the distal epiphysis has a thick and rounded medial lip of the trochlea, caudocranially oriented and coinciding with the distal tip of the humerus. The rounded capitulum and the

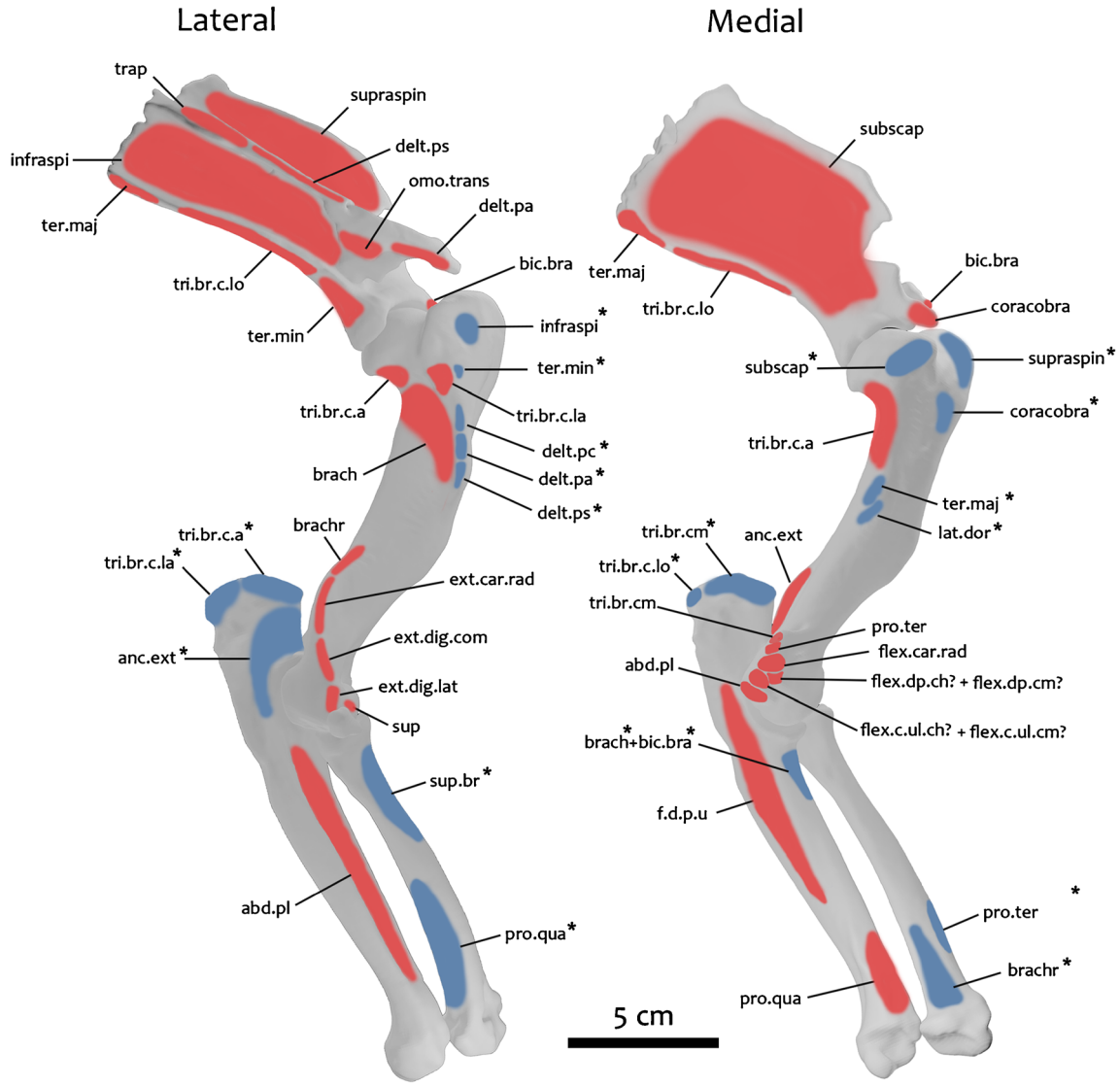

Fig. 4 Illustration of the muscle origin (red) and insertions (blue, and marked with *) based in right scapula MNHN-Bol-V 12617, and right humerus, ulna and radius MNHN-Bol-V 12687. Abbreviations: *abd.pl*, abductor digiti I longus (m. abductor pollicis longus); *anc.ext*, anconeus externum; *bic.bra*, biceps brachii; *brach*, brachialis; *brachr*, brachioradialis (m. supinator longus); *coracobra*, coracobrachialis; *delt.pa*, m. deltoideus pars acromialis; *delt.pc*, m. deltoideus pars clavicularis; *delt.ps*, m. deltoideus pars scapularis; *ext.car.rad*, extensor carpi radialis; *ext.dig.com*, extensor digitorum communis; *ext.dig.lat*, extensor digitorum lateralis; *f.d.p.u.*, flexor digitorum profundus caput ulnare; *flex.c.ul.ch?*, flexor carpi ulnaris caput humerale (possibly); *flex.c.ul.cm?*, flexor carpi ulnaris caput mediale (possibly); *flex.car.rad*, flexor carpi radialis; *flex.dp.ch?*, flexor digitorum profundum caput humerale (possibly); *flex.dp.cm?*, flexor digitorum profundum caput mediale (possibly); *infraspi*, infraspinatus; *lat.dor*, latissimus dorsi; *omo.trans*, omotransversarius; *pro.qua*, pronator quadratus; *pro.ter*, pronator teres; *subscap*, subscapularis; *sup*, m. supinator (m. supinator brevis); *supraspin*, supraspinatus; *ter.maj*, teres major; *ter.min*, teres minor; *trap*, trapezius; *tri.br.c.a*, triceps brachii caput accesorium; *tri.br.c.la*, triceps brachii caput lateralis; *tri.br.c.lo*, triceps brachii caput longum; *tri.br.cm*, triceps brachii caput medialie accessorium (m. epitrocleo-anconeus, or m. anconeus internus)

trochlea are continuous structures. Proximal to the capitulum there is a wide supratrochlear foramen. Medially, the medial epicondyle is broad, massive, and proximodistally oriented. Combined entheses of the main flexors of the forearm originate there (Fig. 6). Proximal to the entepicondyle appears a wide, proximodistally oriented entepicondylar foramen for the medial nerve and brachial artery (Cattoi 1943; Landry 1958). The most proximal facet of the entepicondyle is for the caput mediale accesorium of the m. triceps brachii (m. epitrocleo-anconeus or m. anconeus internus; Taylor 1978; Fisher et al. 2009; Ercoli et al. 2014). Distal to this is the m. pronator teres, and caudal to it is an oval surface for the m. flexor carpi radialis. Distally is an irregular surface assumed to host the origin of the caput humerale and mediale of the m. flexor digitorum profundum. Distal to it, in an oval surface, would lay the caput humerale and caput mediale of the m. flexor carpi ulnaris. The broad and massive origin area, completely distally oriented, is for the m. palmaris longus flexor, which flexes the carpals and

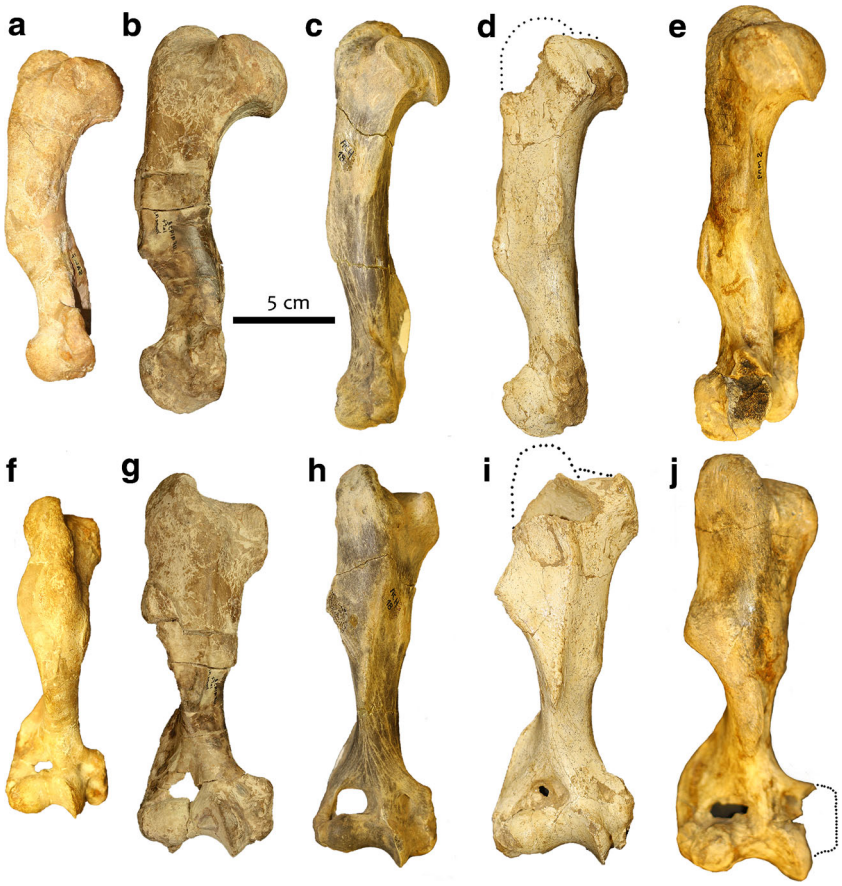

Fig. 5 Comparison for humeri of Mesotheriidae. **a**, **f**, Left humerus of *Trachytherus alloxus* (MNHN SAL 7, mirror image). **b**, **g**, Left humerus of *Trachytherus alloxus* (UF 91933, mirror image). **c**, **h**, Right humerus of *Plesiotypotherium achirense* (paratype, MNHN ACH 18). **d**, **i**, Right humerus of *Plesiotypotherium casirense* (holotype, MNHN-Bol-V 3724). **e**, **j**, Right humerus of *Mesotherium cristatum* (holotype, MNHN PAM 2). **a**-**e**, Top row, images in medial view. **f**-**j**, Bottom row, images in cranial views. The images **b** and **g** are used with permission of FLMNH

the proximal phalangeal joints (Fig. 6; Waibl et al. 2005). The origin area for the m. anconeus (m. anconeus externum) is caudal to the epicondylar crest (crista supracondylaris lateralis) and it lays proximolateral to the supratrochlear foramen.

Ulna

The ulna is long and slender transversely, with a widened distal epiphysis. In lateral view (Fig. 7b), the caudal border is markedly convex, while the cranial border distal to the trochlear notch is straight. The olecranon is well developed, mediocranially oriented, with the proximal border of the olecranon caudocranially expanded (Fig. 7h). The massive proximal tubercle (tuber olecrani) has a rough surface for the attachment of the different folds of the m. triceps brachii: medially, a deep depression marks the origin of the medial head, cranially, the insertion area for the caput accesorium, and caudally, the caput lateralis (Fig. 5). The broad insertion for the m. anconeus is located in the lateral part of the olecranon, proximal to the trochlear notch. Lateral to the ulnar body, there is a transverse depression for the attachment of the m. abductor digiti I longus (m. abductor pollicis longus). In cranial view (Fig. 7h), the trochlear notch is laterally oriented due to the orientation of the anconeus process. The incisura radialis is markedly flat in the parasagittal plane. Distal to the coronoid process appears the attachment for the m. brachialis and m. biceps brachii. The pronator quadratus originates from a broad and triangular facet located cranially in the distal epiphysis. The ulnar body width is slender, while the distal epiphysis is inflated (Fig. 7h). In medial view, the origin for the caput mediale accesorium of the m. triceps brachii occupies the proximal border of the olecranon; in the medial part of the ulnar body, a triangular and longitudinal depression coincides with the insertion for the caput ulnare of the m. flexor digitorum profundus. The circunferentia articularis is oval and connects with the incisura ulnaris of the radius. Distocranially, the facies articularis carpi radii contacts the pyramidal and the pisiform.

Radius

The radius is flattened distocranially with well-developed radial head and distal epiphysis. The diaphysis is oval in cross section all along the bone. The proximal articular surface is oval and mediolaterally enlarged. It presents two depressed areas: the fovea capitis radii (lateral), facing the rounded trochlea humeri, and another one on the medial border, facing the capitulum. The dorsal border is rounded and continuous. In cranial view (Fig. 8b), the neck is elongate mediolaterally and flattened craniocaudally. The distal portion displays grooves for three tendons: for the m. abductor digitis I in the medial border, for the m. extensor carpi radialis just lateral to it, and finally for the m.

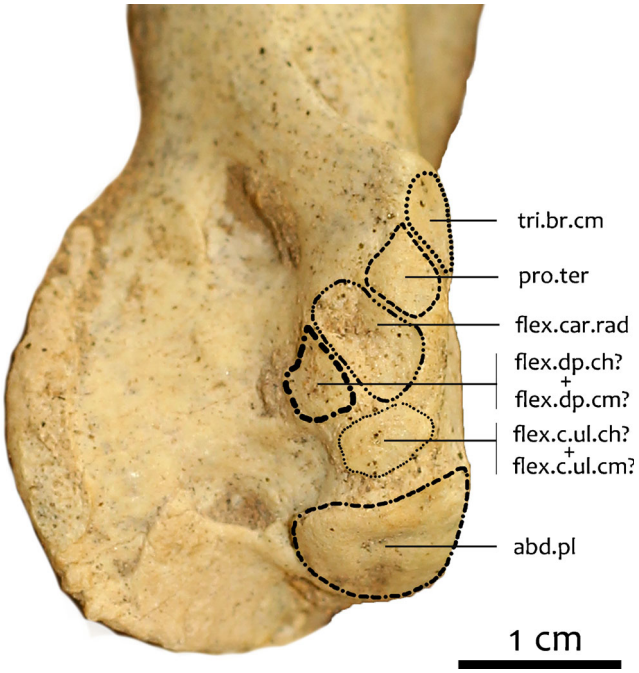

Fig. 6 Lateral entepicondyle of the right humerus of *Plesiotypotherium achirense* (MNHN-Bol-V 12987) showing the attachment of the main flexor muscles of the forearm. Abbreviations: *abd.pl*, abductor pollicis longus; *flex.c.ul.ch?,* flexor carpi ulnaris caput humerale (possibly); *flex.c.ul.cm?,* flexor carpi ulnaris caput mediale (possibly); *flex.car.rad*, flexor carpi radialis; *flex.dp.ch?,* flexor digitorum profundum caput humerale (possibly); *flex.dp.cm?,* flexor digitorum profundum caput mediale (possibly); *pro.ter*, pronator teres; *tri.br.ca*, triceps brachii caput mediale accesorium

Fig. 7 Comparison of ulnae of Mesotheriidae. **a**, **g**, Left ulna of *Trachytherus alloxus* (UF 91933, mirror image). **b**, **h**, Right ulna of *Plesiotypotherium achirense* (MNHN-Bol-V 12687). **c**, **i**, left ulna of *Plesiotypotherium casirense* (holotype, MNHN-Bol-V 3724). **d**, **j**, Right ulna of *Pseudotypotherium* sp. (MACN 7972). **e**, **k**, Right humerus of *Mesotherium cristatum* (holotype, MNHN PAM 2). **a**-**e**, Top row, images in medial view. **g**-**l**, Bottom row, images in cranial view. The images **a** and **g** are used with permission of FLMNH

extensor digitorum communis. In lateral view (Fig. 8f), the supinator muscle (m. supinator brevis) inserts in a concave surface distal to the radial head (Fig. 4). Distal to it is a depressed surface proximodistally elongated and located in the distal half of the shaft, which hosts the insertion for the m. pronator quadratus. In medial view (Fig. 8), in the distal epiphysis is a triangular insertion for the m. brachioradialis (Fig. 4). In dorsal view (Fig. 3d), the wide oval articular facets for the scaphoid and the lunar are visible distally. In distal view, distal to the neck appears the inflated surface of the bicipital tuberosity where the tendon for the m. biceps brachii inserts (Fig. 8f).

Manus

The manus of *Pl. achirense* is pentadactyl with bifid ungual phalanges (Villaroel 1974). The first digit is slender with a markedly slenderer Mc I. The largest metacarpal is the Mc II. Yet, in anatomical position, the Mc III reaches a more distal position than any other metacarpal (Fig. 9). The proximal phalanges of digits II-III are robust proximally and tapering/narrowing distally. Median phalanges show a similar pattern, although less pronounced. The phalanges show a palmar articular facet for a large sesamoid preventing the over extension of the digits (Shockey et al. 2007). Distal phalanges are bifid, with a deep median sagittal groove. Their height regularly diminishes distally, whereas their width increases. In dorsal view, in anatomical position the metacarpals have a fan-shaped pattern, as in other mesotheriids (see Shockey et al. 2007; Cerdeño et al. 2012), similar to what is observed in ursids or other terrestrial carnivorans.

Comparative Anatomy

Scapula

The scapula of *Pl. achirense* is rectangular in lateral view, with slender scapular spine, fossa infrascapularis, and fossa supraspinata with respect to those of *Mesotherium cristatum*. The area of the cavitas glenoidale is lower in *Pl. achirense* than in *Pseudotypotherium* sp. or in *Mesotherium* due to a larger proximal projection of the tuberculum supraglenoidale in the latter taxa. Shockey et al. (2007) described a high scapular

spine for *Trachytherus alloxus*. The same pattern is observed for the massive scapula of *M. cristatum* with the presence of a broad postscapular fossa, similar to that of ursids (including *Ailuropoda*; Davis 1964) or amphicyonid carnivorans (Davis 1949). Serres (1867) indicated for *M. cristatum* that the distance between the coracoid process and the hamatus process determines a wide muscular insertion area. In *Pl. achirense* and *M. cristatum* the hamatus process is equally proximally projected, while the suprahamatus process is notably proximally oriented in *M. cristatum*, and enlarged caudally in *Pl. achirense.*

Humerus

The humerus of *Pl. achirense* is slenderer than that of *Trachytherus alloxus*, *Plesiotypotherium casirense*, *Pseudotypotherium* sp. and *Mesotherium cristatum* (HRI, see Table 2). The greater trochanter in *Pl. achirense* is not as wide as in *M. cristatum* or in *T. alloxus*. The humerus of *T. alloxus* MNHN SAL 7 (Fig. 5a, f) is not informative because the deltoid crest is restored. The humerus of *T. alloxus* is more massive than in *Pl. achirense* mainly in the proximal epiphysis, the entepicondyle, and the trochlea. *Plesiotypotherium casirense* show the highest EI values for any mesotheriid included in the comparison sample (see Table 2). In medial view (Fig. 5a–e), the distal border of the humeral head does not project as far over the

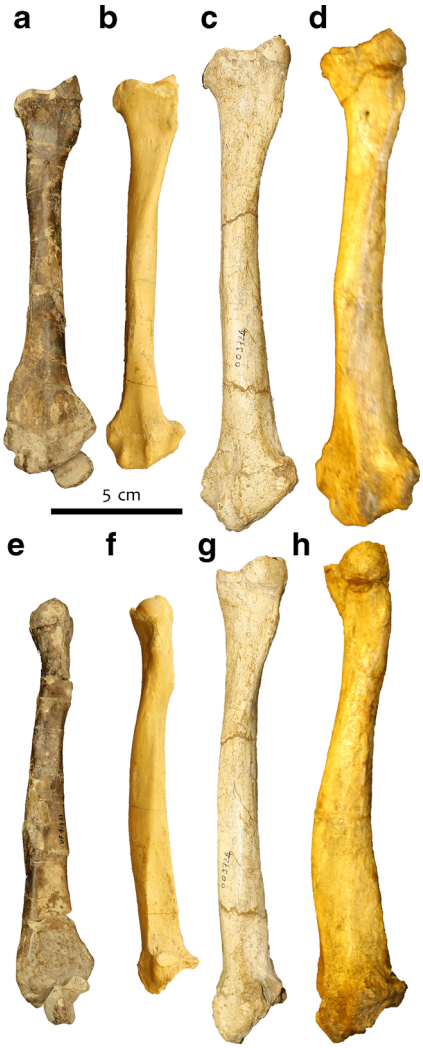

Fig. 8 Comparison for radii of Mesotheriidae. **a**, **e**, Left radius of *Trachytherus alloxus* (UF 91933). **b**, **f**, Left radius of *Plesiotypotherium achirense* (holotype, MNHN-Bol-V 12687). **c**, **g**, Left radius of *Plesiotypotherium casirense* (MNHN-Bol-V 003724). **d**, **h**, Left radius of *Mesotherium cristatum* (holotype, MNHN PAM 2). **a**-**d**, Top row, images in cranial view, **e**-**h**, Bottom row, images in lateral view. The images **a** and **e** are used with permission of FLMNH

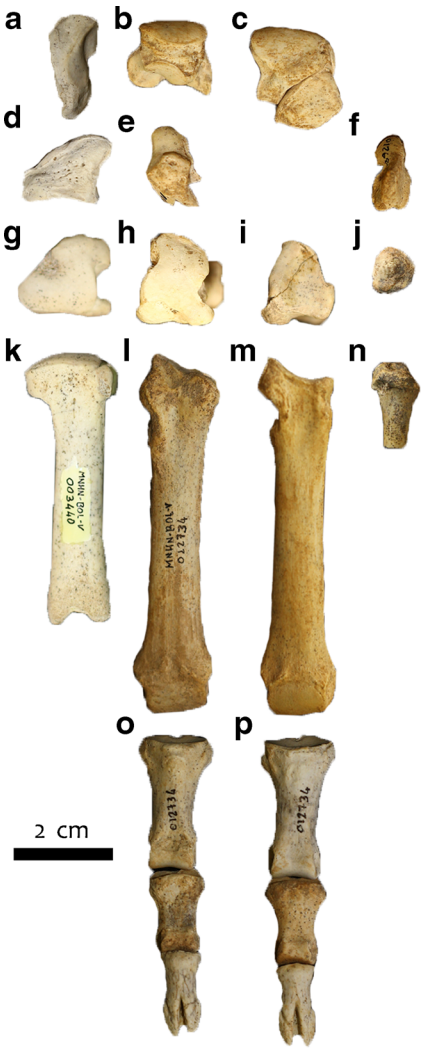

Fig. 9 Carpals and metacarpals of *Plesiotypotherium achirense*. **a**, Right pyramidal (MNHN-Bol-V 12734). **b**, Right semilunate (MNHN-Bol-V 12687). **c**, Right scaphoid and trapezoid (MNHN-Bol-V 12687). **d**, Right unciform (MNHN-Bol-V 12734). **e**, Right pyramidal (MNHN-Bol-V 12687). **f**, Right trapezium (MNHN-Bol-V 12687). **g**, Right Mc IV (MNHN-Bol-V 3440). **h**, Right Mc III (MNHN-Bol-V 3443). **i**, Right Mc II (MNHN-Bol-V 12687). **j**, Right Mc I (MNHN-Bol-V 3444). **k**, Right Mc IV (MNHN-Bol-V 3440). **l** Right Mc III (MNHN-Bol-V 12734). **m**, Right Mc II (MNHN-Bol-V 12687). **n**, Right Mc I (MNHN-Bol-V 3444). **o**, **p**, Sequential three phalanges of finger III and IV, respectively. **a**-**f**; **k**-**p**, dorsal views. **g**-**j**, proximal views

humeral neck in *Pl. achirense* as in *T. alloxus*, *Pl. casirense*, or *M. cristatum*. The proximal half of the diaphysis is straight in *Pl. achirense*, *Pl. casirense* (more massive), and *M. cristatum* (slenderer), while the humeral head and the proximal diaphysis are caudally displaced in *T. alloxus*. The crista supracondylaris lateralis is curved in all studied taxa; however, the mediolateral border is flat in *Pl. casirense*. The subscapularis facet origin is slightly marked in *T. alloxus*, while it is inflated in other taxa, wider in *Pl. casirense*, and even wider in *M. cristatum*. In cranial view (Fig. 5f–j), the lateral tip of the tuberositas deltoidea has similar heights in *T. alloxus*, *Pl. achirense*, and *Pl. casirense*, while it is located more distally (closer to the half of the humeral body) in *M. cristatum* (Fig. 5). In the last taxon, there is a marked change of angle for the lateral borders of the crista humeri and crista tubercularis majoris with respect to other taxa. The epicondylus medialis, the epicondylus lateralis, and the crista supracondylaris lateralis are more massive in *Pl. casirense* and still more in *M. cristatum* than in *Pl. achirense*. The curvature of the crista supracondylaris lateralis is similar in both *Plesiotypotherium* species and in *C. munozi*, while in *M. cristatum* this lateral border is straight. The supratrochlear foramen is wide, circular, and laterally oriented in all specimens referred to as *Pl. achirense*, while in *T. alloxus*, *Pl. casirense*, and *M. cristatum* there is an oval fossa radialis (not open) located medially.

Ulna

The main ulnar differences are in their curvatures, olecranon extension, and muscular insertions surfaces. In medial view (Fig. 7 a–f), the cranial border of the ulnar body is straight and the dorsal border is concave. In lateral view, the caudal border of the ulnar body reaches the level of the trochlear notch in *T. alloxus*, *Pl. achirense*, *Pl. casirense*, and *Pseudotypotherium* sp., whereas it is at mid-height of the ulnar body in *M. cristatum*. The olecranon is higher in *T. alloxus* and in *M. cristatum* than in *Pl. achirense*. In this last taxon and also in *Caraguatypotherium munozi* and *M. cristatum*, the olecranon is expanded craniodorsally. There is variation in the olecranon curvature and expansion in the two available ulnae of *M. cristatum*: MACN 6875 is cranially curved and MNHN PAM 2 is not curved but craniodorsally expanded. The index of fossorial ability (IFA, see Table 2) is highest for *M. cristatum* (IFA=34.53), followed by *Pl. achirense* (IFA=32.91), and finally *C. munozi* (IFA=30.64) and *Pl. casirense* (IFA=30.78), which have similar values. The ulna robustness index (URI, see Table 2) indicates a major value for *Pl. achirense*, followed by *M. cristatum*, and finally *Pl. casirense* and *C. munozi*. The ulnar body is wide craniodorsally and the facies articularis carpi is mediolaterally enlarged in *M. cristatum* with respect to the other included taxa. In lateral view, the proximal part of the trochlear notch is oriented transversely in *Pl. achirense* and in *Pl. casirense* but not in other taxa, which show a cranioproximal orientation. In cranial view (Fig. 7g–l), the distal part of the trochlear notch forms a wide, oval surface in *Pseudotypotherium* sp. (Fig. 7j) and in *M. cristatum* (Fig. 7k, l), whereas it seems to be a continuous surface in *T. alloxus* (Fig. 7g), *Pl. achirense* (Fig. 7h), and *Pl. casirense* (Fig. 8i).

Radius

Radii have a similar gross morphology in all taxa compared. The radial robustness index (RRI; see Table 2) is similar in *C. munozi, Pl. achirense*, and *M. cristatum*. And for a similar size (e.g., no allometric comparison), the radius distal epiphysis of *T. alloxus* is more robust mediolaterally and caudocranially. *Plesiotypotherium casirense* has the most robust radius, further thickening distally from the mid-diaphysis. Radii of all studied mesotheriines show a marked curvature in lateral (Fig. 8a–d) and medial views, which is much weaker in the trachytheriine *T. alloxus*. The radial neck in mesotheriids is oval in cross section. In lateral view, the radius of *Pl. achirense* and *T. alloxus* has a deep triangular insertion area for the m. pronator quadratus, contrary to what is observed in *Pl. casirense* and *M. cristatum* (Fig. 8e–h). The radius of *C. munozi* is similar to that of *Pl. achirense*. In cranial view (Fig. 8a–d), the distal epiphysis of *T. alloxus* shows a well-marked lateral groove for the extensor digitorum. This feature is not so developed in mesotheriines. A radial sesamoid is attached to the radius and the humerus of the articulated forelimb of MNHN-Bol-V 12687 (Fig. 7g).

Manus

The manus of *Pl. achirense* seems to be much slenderer than in the other mesotheriids compared (*T. alloxus, Pl. casirense*, and *M. cristatum*) regarding carpals, metacarpals, and phalanges. The carpals are wider (mediolaterally) in *M. cristatum* and *T. alloxus*, than in both *Plesiotypotherium* species compared.

In cranial view, the lateral and medial edges of the metacarpals in *T. alloxus*, *Pl. achirense*, and *Pl. casirense* are straight, whereas they are concave in *M. cristatum*. The pisiforms are more robust in *Pl. casirense* than in the other studied taxa.

Discussion

Scapulo-Humeral Joint

The scapular girdle is complete. The presence of a clavicle (although plesiomorphic at the mammaliaform level; Kielan-Jaworowska et al. 2004) and of wide insertion areas for the m. supraspinatus and m. infraspinatus might have helped stabilize the shoulder humeral joint, minimizing dislocation forces. The rectangular shape of the scapula is similar to that observed in

the terrestrial didelphimorphians *Metachirus* and *Didelphis* (Argot 2001). The bifurcation of the acromion plate into a processus hamatus and processus suprahamatus (metacromion process), as observed for example in the carnivorans *Procyon* and *Nasua nasua* (procyonids), *Arctictis binturong* (viverrid), and *Puma concolor* (felid), or the capybara *Hydrochoerus*, a rodent, is considered a plesiomorphic character within Eutheria (Meng et al. 2003). According to Shockey et al. (2012), a recessed metacromion and a beaked acromion as seen in *Pl. achirense* and in *M. cristatum* are considered synapomorphic traits within Notoungulata, while an extended acromion is symplesiomorphic. The coracoid process (Fig. 2a–c) is the insertion for the m. coracobrachialis, while the pars clavicularis (m. cleidobrachialis) inserts on the clavicle. Caudally, the m. biceps brachii inserts on the tuberculum supraglenoidale, which is ventrally directed in *M. cristatum* in comparison with *Pl. achirense*. This orientation would have helped for the flexion movement of this muscle and for a better contact with the humeral head, which would in turn stabilize the scapulo-humeral joint in *M. cristatum*. The scapulae of *Pl. achirense* show a small postscapular fossa. Yet, in *M. cristatum* the insertion of the m. teres major is both well developed, as observed in ursid carnivorans (Davis 1949), and caudodistally projected (Fig. 10a,b), which would increase the lever arm of the m. teres major (Maynard Smith and Savage 1956; Argot 2001), providing a powerful humeral retraction (Hildebrand 1985; Kley and Kearney 2007). The m. teres major then acts as a flexor, together with the m. triceps brachii caput longum, and caput laterale.

The general shape of the humerus in lateral and medial views is similar to that of the carnivorans *Nasua nasua*, and *Lutra lutra*, and somewhat recalling that of the large rodents *Hydrochoerus* sp. and *Cuniculus paca* for the proximal epiphysis. Mesotheriids have neither the extremely developed and medially displaced entepicondyle of the wombat *Vombatus ursinus*, or the anteater *Tamandua* sp., nor the high developed deltopectoral crest of *Vombatus ursinus* or the porcupine *Hystrix cristata*. In *Pl. achirense* and in the mesotheriids compared, the humeral head is ball-shaped, which would be related to the facilitation of adduction movements. On the other hand, the high development of the great tubercle, as observed in all the mesotheriids compared, would limit the abduction and extension movements of the scapula-humeral joint, accordingly restricted to the parasagittal plane (Argot 2001; Polly 2007; Candela and Picasso 2008). This feature increases the need for stabilization of the shoulder in scratch-diggers (Szalay and Sargis 2001). The small caudolateral development of the bicipital tuberosity of the radius, observed in all mesotheriids, would point to a weak m. biceps brachii (Argot 2001, 2012).

The deltoid crest, the m. deltoideus pars acromialis, pars scapularis, and pars spinalis are strongly developed. The m. pectoralis major and the m. deltoideus pars clavicularis act as adductors. Powerful pectoral muscles are required for adduction movements, as in fossorial (*Ctenomys* sp.), semifossorial (*Euryzygomatomys* sp. and *Carterodon* sp.), arboreal (porcupines), or semiaquatic rodents (*Myocastor coypus*; Candela and Picasso 2008). The hamatus process in which the m. deltoideus pars acromialis inserts is elongated ventrocranially and convex medially in the mesotheriids *Pl. achirense, Pseudotypotheirum* sp., and *M. cristatum*. It is not as extremely developed as in *Tamandua*, but this conformation may help the m. deltoideus pars acromialis for the protraction or abduction of the humerus (Taylor 1978). When the m. deltoideus is well developed, in all mesotheriids, the pars scapularis acts as a flexor muscle. In *M. cristatum*, the deltoid crest is distally oriented, which allows an increased moment arm for the m. deltoideus and the m. pectoralis and improves the adduction of the humerus (Fig. 10a,b).

Humero-Ulnar and Humero-Radial Joint

In caudal and cranial views, the distal half of the humerus of the studied mesotheriids is similar to that of extant mammals with a semifossorial behavior, such as the American badger (*Taxidea* sp.; Shockey et al. 2007). Main similarities are wide entepicondyle and ectepicondyle and a marked crista supracondylaris lateralis (supinatory crest). This crest allows a large attachment surface for the m. brachioradialis, the m. extensor carpi radialis, and other wrist and finger muscles (Salesa et al. 2008). Abductors play an indisputable locomotory role, as inferred by the presence of a wide insertion area for the m. abductor digiti I longus in the lateral side of the ulna.

In the entepicondyle, which is wide, massive, and proximodistally elongated, are located the origin for several flexor muscles (Fig. 6). The m. triceps brachii caput mediale accesorium (m. epitrochleo-anconeus and m. anconeus internus) inserts on the medial side of the olecranon. As observed in the elbow joint of the anteater *Tamandua* sp. and the marsupial *Didelphis* sp., the presence of large torques in these cases may be explained by a muscular rather than by an osteological mechanism (Taylor 1978). We hypothesized the same mechanism for mesotheriids. In mesotheriids the presence of the m. anconeus and m. triceps brachii caput mediale accesorium is inferred; both act to pull the olecranon either laterally or medially, which results in adduction or in abduction, respectively, and therefore stabilizes the elbow. In this sense, the epicondyle index (EI, see Table 2) is higher for *Pl. casirense* (EI=37.55) than for any other mesotheriid compared (32.30-37.55), and is related with extension forces of the elbow. Other biological indices recovered are consistent with fossorial abilities (HRI>30 and BI(r)<90; see Table 2), as indicated by Shockey et al. (2007). According to Candela and Picasso (2008), a robust entepicondyle may help flexion movements in arboreal animals, such as the rodent

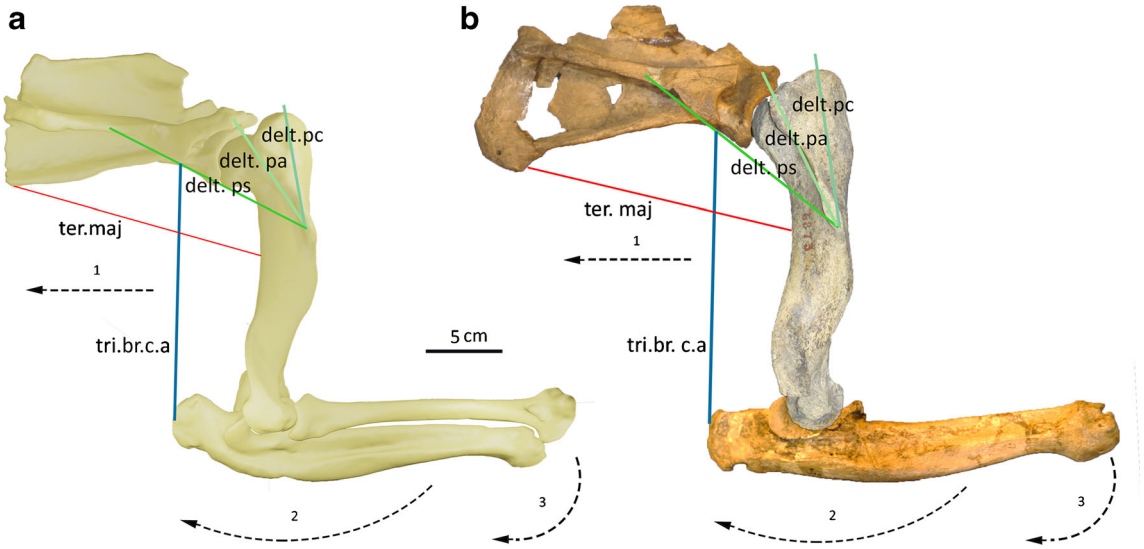

Fig. 10 Schematic of action lines while digging. **a**, Action lines of muscles for *Plesiotypotherium achirense* (right scapula MNHN- Bol-V 12617; right humerus, ulnae and radius MNHN-Bol-V 12678). **b**, Action lines for *Mesotherium cristatum* (derived condition; right scapula and ulna MNHN PAM 2; right humerus MACN 6873). Abbreviations: *delt.pa*, pars acromialis m. deltoideus; *delt.pc*, pars clavicularis m. deltoideus; *delt.ps*, pars scapularis m. deltoideus; *ter.maj*, teres major muscle; *tri.br.c.a*, caput longum triceps brachii muscle; 1 limb retraction; 2 elbow extension; 3 wrist flexion

Dactylomys sp., and stabilize the humero-radial joint in scratch-diggers such as living porcupines (McEvoy 1982). In medial view, the ulna of mesotheriids have a marked m. flexor digitorum profundus, which, together with the well-developed entepicondyle, is evidence for a high flexion activity for this muscle as in the extinct condylarth *Arctocyon primaevus* (Argot 2012). The medial lip of the trochlea is distally elongated in all studied mesotheriids, except *T. alloxus* (Fig. 5f–j). The distally elongated medial lip of the trochlea prevents the dislocation of the elbow from transversal constraints. A lateral radial sesamoid of the elbow is evidenced in *T. alloxus*, *C. munozi*, *Pl. achirense,* and *Pl. casirense*. As discussed by Shockey et al. (2007) for *T. alloxus*, the specific function of this sesamoid is unknown, but it may have stabilized the joint and somewhat impeded dislocation of the elbow. The olecranon of all taxa compared here is wide mediolaterally and medially oriented, with rough surfaces for the insertion of the m. triceps brachii and the m. anconeus. And, therefore, extension movements were favored in all concerned mesotheriids. An elongated olecranon implies a well-developed m. triceps brachii and therefore a marked extension of the forearm (Argot 2001). Regarding the m. anconeus, many other functions are suggested, such as stabilizing the joint and avoiding joint flexion in static position (Ercoli et al. 2014). This muscle is well developed in diggers and climbers (see Ercoli et al. 2014).

The crista supracondylaris lateralis is well developed, and is associated with attachment of the extensor muscles (e.g., m. extensor carpi ulnaris) and of the m. supinator brachioradialis. In *Tamandua* sp., this latter muscle attachment has migrated proximally (Taylor 1978). This condition is not so marked in mesotheriids; it is more similar to what is observed in *Didelphis* sp. with a developed m. brachioradialis and therefore a noticeable supinatory activity. In highly specialized fossorial animals, such as the armadillo *Dasypus* sp., there is no particular development of the m. brachioradialis, and supinatory activity is restricted (Olson et al. 2015).

The trochlear notch of the ulna is open in mesotheriids, which is related with wide movements of extension-flexion of the elbow (Argot 2001). Regarding the flexion and the extension of the elbow, there is a marked angle between the transversal planes of the humerus, ulna, and radius. The maximum extension of the elbow is ca. 120°, while the flexion is ca. 25-30°, as estimated under extreme supination of the hand. Supination and pronation movements were favored, as inferred by the presence of free unfused ulna and radius and of a hemispherical capitulum humeri (Szalay and Dagosto 1980; Rose 1993). The m. pronator quadratus is well developed, with broad insertions on both the ulna and radius, especially in *T. alloxus* and in *Pl. achirense*; this muscle is known to act at stabilizing both bones (Argot 2001). The protruding entepicondyle indicates a strong development of the other pronator muscle, the m. pronator teres, which is consistent with massive flexors.

Powerful limb flexion, in order to keep the center of gravity close to the substrate and therefore to increase the stability and control of the movement, is shared in some digging and climbing taxa (Argot 2001; Ercoli et al. 2014). In mustelids, the development of extensors exceeds that of flexors, especially in digging mustelids (Ercoli et al. 2014). To sum up, the

flexor and extensor muscles were strongly developed in this joint, and therefore flexion-extension movements were highly favored in mesotheriids as is typical for fossorial mammals (EI, see Table 2). Accordingly, supination-pronation movements, which are common in semifossorial animals (Ercoli et al. 2014), but not in highly specialized placentals such as moles, armadillos, and pangolins (Polly 2007), are inferred.

Wrist Joint

Proximal carpals (lunar and scaphoid) with proximally concave surfaces indicate good rotation capabilities with the forearm (radius and ulna) as in *T. alloxus*, *Pl. achirense*, *Pl. casirense*, *Pseudotypotherium* sp., and *M. cristatum*. Distally, the contact with other carpals forms complex and interlocking unions. The proximal parts of the Mc III-IV are in tight contact with those of adjacent carpals, and form non-rotatory unions, except for Mc IV (Fig. 9g–i). Precise control of individual digits is not necessary for scratch-digging behaviors (Olson et al. 2015) and on the other hand, a unique structure that acts as a shovel would support better large stresses during digging activity, as observed in highly specialized diggers such as moles (Hildebrand 1985). The metacarpals are strongly convex distally, which would indicate wide rotation movements at the metacarpal–proximal phalanges transition (in the parasagittal plane), and therefore efficient flexion/extension movements of each stroke in digging. The ungual phalanges are bifid or fissured as in other diggers such as pangolins, armadillos, and moles (Hildebrand 1974; Kardong 2002), and their distal edges are mediolaterally enlarged. Together with the presence of hooves, this would have increased the first contact of the stroke during scratch-digging in all mesotheriids.

Functional Morphology and Forelimb Characteristics of Scratch-Digging Mammals

The common characters shared by scratch-digging mammals and reflected in forelimb skeletal elements (Bou et al. 1990; Hildebrand and Goslow 2001) have been compiled by Rose et al. (2014). They mainly consist of: i) a broad scapula related to high, massive humeral retractor and shoulder joint stabilizer muscles; ii) a robust humerus resisting high bending forces (Quaife 1978; Hildebrand 1985); iii) a prominent medial epicondyle attaching the large carpal and flexor muscles; iv) an elongated olecranon for the extensor elbow muscles (Hildebrand and Goslow 2001); v) a shortened radius; and vi) stout carpals, metacarpals, and phalanges related with sharp claws (Quaife 1978).

Mesotheriids share some of these typical fossorial characteristics: i) robust humerus, ii) well-developed entepicondyle, iii) elongated olecranon, iv) shortened radius, v) strong manus with robust carpals and phalanges, and vi) bifurcated and sharp claws. The inferred functional properties, based on comparison with extant mammals with similar bones or osteological structures, help us to make an accurate myological reconstruction, and therefore infer a digging lifestyle.

According to the compared osteological features and the functional properties inferred for Mesotheriidae, we consider *M. cristatum* as the most derived representative taxon for a typical scratch-digger mesotherid lifestyle.

The inferred functional properties (see sections above) for mesotheriids were found to be consistent with a digging faculty and the postcranium shares similarities with animals that have such functional abilities, such as the mustelid *Taxidea*, the procyonid *Nasua*, and the orycteropodid *Orycteropus* (Patterson 1975; Gomper 1995; Michener 2004). Scratch-digging activity is mainly made with rapid movements, and using alternatively left and right forefeet (Holliger 1916; Hickman 1985). These movements are mainly within the parasagittal plane. Locomotor activities in some scratch-digging animals, such as rodents, are made mainly using the forefeet, but in some cases, incisors may help for substrate removal (Agrawal 1967; Lessa and Thaeler 1989; Lessa and Stein 1992; Ebensperger and Bozinovic 2000; Stein 2000).

Regarding other lifestyles, cursoriality (adaptation for running in open spaces; Gregory 1912) coincides with reduction of lateral digits that decrease the area of support (e.g., in perissodactyls and artiodactyls; Gambaryan 1974). Natatorial mammals and semifossorial mammals share: i) a long olecranon, ii) a developed entepicondyle, and iii) high pectoral muscles developing high abduction movements (Polly 2007). Mesotheriids have short and robust phalanges, contrary to natatorial specialists (long manus with long digits). Similarly, scansorial mammal limbs are often elongated, with distal phalanges having long, curved claws, and rotatory shoulders (Cartmill 1974).

Conclusions

Our morpho-functional reconstruction of the forelimb of mesotheriids allows for inferring independently the muscular pattern and the origin/insertion areas for the concerned muscles. We infer an unambiguous scratch digging faculty for mesotheriids from the form-function complex as observed on the forelimb.

Forelimb features of *Plesiotypotherium achirense* are consistent with a scratch digging faculty:

1) There is good stabilization of the shoulder–humeral joint, primarily because of the strong muscle configuration (m. infraspinatus, m. supraspinatus, m. subscapularis, and m. coracobrachialis), but also due to the structural bony configuration (proximal orientation of the greater trochanter further limiting extension movements), with a complete scapular girdle, a high scapular spine, an enlarged acromion, and a well-developed deltoid crest.

2) The humero-ulnar and humero-radial joints are widely enlarged, with well-developed entepicondyle, ectepicondyle, and supracondylaris crest, a medial lip of the trochlea distocranially oriented, the presence of an elbow sesamoid, and an enlarged olecranon. Contrary to what is observed in highly specialized fossorial mammals, *Pl. achirense* has free and independent ulna and radius and an oval radial head, allowing for wide pronation-supination movements.
3) The manus is strong, with robust carpals, metacarpals, and phalanges. Ungual phalanges are mediolaterally elongated and bifid, as in all mesotheriids.

Bony features, biological indices, and muscular patterns analyzed here provide key information about the form-function complex for the forelimb of Mesotheriidae:

1) The shoulder–humeral joint is strongly stabilized with mainly flexor muscles (m. deltoideus, m. teres major, and m. teres minor), and adductor muscles (m. infraspinatus).
2) The humero-ulnar and humero-radial joint shows well-developed extensor (m. triceps brachii), supinator (m. brachioradialis and m. supinator brevis), and pronator muscles (m. pronator teres and m. pronator quadratus). Enlarged entepicondyle and ectepicondyle receive well-developed flexors and extensors, respectively.

Accordingly, muscular capacities of mesotheriids were likely to generate significant out-forces against the substrate (see Shockey et al. 2007), during (i) limb retraction, (ii) elbow extension, and (iii) wrist flexion (Fig. 10a,b), consistent with typical functional complexes of inferred scratch-diggers. This scratch-digging ability was most likely still augmented in *M. cristatum*, as indicated by osteological configurations, while biological robustness indices (HRI, URI, and RRI, see Table 2) have similar values in other mesotheriines. *Mesotherium cristatum* further differs from other mesotheriids in having (i) a caudally displaced distal border of the scapula (likely to have increased the moment arm of main flexor muscles of the shoulder-humeral joint) where the suprascapular fossa for the m. teres majus inserts, (ii) a massive deltoid crest, more distally located and laterocaudally oriented, and (iii) a proximal crista supracondylaris lateralis laterally projected on the humerus.

Acknowledgments We thank A. Kramarz and S. Alvarez (MACN, Buenos Aires, Argentina), C. de Muizon, C. Argot, and G. Billet (MNHN, Paris, France), and D. Rubilar (SGOPV, Santiago, Chile) who kindly gave access to the specimens under their care. We are grateful to R. C. Hulbert. Jr (FLMNH, Gainesville, USA) for sending and allowing us to reproduce images of *Trachytherus alloxus* (UF 91933) and to D. A. Croft for providing measurements of this specimen.

We thank all the team members (M. A. Abello, S. Adnet, G. Billet, L. Marivaux, M. B. Prámparo, P. Münch, and R. Andrade Flores) who participated in the collecting of the specimens from Achiri in 2010–2015). We are grateful to N. Toledo for helpful discussions on an earlier version of the manuscript. Finally, we thank MEDICENTRO clinic of La Paz (Bolivia) for providing us access to their computed tomography facility.

We warmly thank people from Achiri for facilitating our fieldwork (2010–2015). This work was partially funded by ECOS-FonCyT (A14U01). This project was made possible thanks to the cooperation agreement between the MNHN-Bol (Bolivia), the ISEM (France), and the CONICET (Argentina, CONICET Cooperation agreement N°864/2014).

References

Agrawal VC (1967) Skull adaptations in fossorial rodents. Mammalia 31: 300-312

Ameghino F (1889) Contribución al conocimiento de los mamíferos fósiles de la República Argentina. Acad Nac Cienc Córdoba 6:918-919

Ameghino F (1891) Observaciones sobre algunas especies de los géneros *Typotherium* y *Entelomorphus*. Rev Arg Hist Nat: 1:433-437

Argot C (2001) Functional-adaptative anatomy of the forelimb in the Didelphidae, and the paleobiology of the Paleocene marsupials *Mayulestes ferox* and *Pucadelphys andinus*. J Morphol 247:51-79

Argot C (2012) Postcranial analysis of a carnivoran-like archaic ungulate: the case of *Arctocyon primaevus* (Arctocyonidae, Mammalia) from the late Paleocene of France. J Mammal Evol 20:83-114

Billet G, Muizon C de, Mamani Quispe B (2008) Late Oligocene mesotheriids (Mammalia, Notoungulata) from Salla and Lacayani (Bolivia): implications for basal mesotheriid phylogeny and distribution. Zool J Linn. Soc 152:153-200

Bond M, Cerdeño E, López G (1995) Los ungulados nativos de América del Sur. Mon Mus Nac Cienc Nat: Cons Sup Inv Cient Madrid 12:257-276

Bou J, Castiella JJ, Casinos A (1990) Multivariate analysis and locomotor morphology in insectivores and rodents. Zool Anz 225:287-294

Candela AM, Picasso MBJ (2008) Functional anatomy of the limbs of Erethizontidae (Rodentia, Caviomorpha): indicators of locomotor behavior in Miocene porcupines. J Morphol 269:552-593

Cartmill M (1974) Pads and claws in arboreal locomotion. In: FA Jenkins Jr (ed) Primate Locomotion. Academic Press, New York, pp 45-83

Cattoi N (1943) Osteografía y osteometría comparada de los géneros *Typotheriodon* and *Typotherium*. Mus Arg Cienc Nat Buenos Aires, 119 pp

Cerdeño E, Vera B, Schmidt GI, Pujos F, Mamani Quispe B (2012) An almost complete skeleton of a new Mesotheriidae (Notoungulata) from the late Miocene of Casira, Bolivia. J Syst Palaentol 10:341-360

Croft DA (2007) The middle Miocene (Laventan) Quebrada Honda Fauna, southern Bolivia and a description of its notoungulates. Palaeontology 50: 277-303

Croft DA, Anderson LC (2008) Locomotion in the extinct notoungulate *Protypotherium*. Paleontol Electron 11:1-20

Croft DA, Flynn JJ, Wyss AR (2004) Notoungulata and Litopterna of the early Miocene Chucal Fauna, northern Chile. Fieldiana Geol 50:1-52

Davis DD (1949) The shoulder architecture of the bears and other carnivores. Fieldiana Zool 31:285-305

Davis DD (1964) The giant panda: a morphological study of evolutionary mechanism. Fieldiana Zool 3:1-339

De Iuliis G, Pulera D (2010) Dissection of Vertebrates: A Laboratory Manual. Elsevier/Academic Press, Amsterdam

Ebensperger LA, Bozinovic F (2000) Energetics and burrowing behaviour in the semifossorial *Octodon degus* (Rodentia: Octodontidae). J Zool 252:179-186

Elissamburu A, Vizcaíno SF (2004) Limb proportions and adaptations in caviomorph rodents (Rodentia: Caviomorpha). J Zool Lond 262:145-159

Ercoli MD, Álvarez A, Stefanini MI, Busker F, Morales MM (2014) Muscular anatomy of the forelimbs of the lesser grison (*Galictis cuja*), and a functional and phylogenetic overview of Mustelidae and other caniformia. J Mammal Evol 22:57-91

Fisher RE, Adrian B, Barton M, Holmgren J, Tang SY (2009) The phylogeny of the red panda (*Ailurus fulgens*): evidence from the forelimb. J Anat 215:611-635

Flynn JJ, Croft DA, Charrier R, Wyss AR, Hérail G, García M (2005) New Mesotheriidae (Mammalia, Notoungulata, Typotheria), geochronology and tectonics of the Caragua area, northernmost Chile. J South Am Earth Sci 19:55-74

Gambaryan PP (1974) How Mammals Run: Anatomical Adaptations. John Wiley and Sons, New York.

Gervais P (1867) Sur une nouvelle collection d'ossements fossiles de mammifères recueillie par M. Fr. Seguin dans la confédération argentine. C R Acad Sci 55:279-282

Gervais P (1869) Zoologie et paléontologie générales: nouvelles recherches sur les animaux vertébrés vivants et fossiles. Librairie de la Société de Géographie, Paris 5:1-56

Gomper ME (1995) *Nasua narica*. Mammal Spceies 487:1-10

Hammer Ø, Harper DAT, Ryan PD (2001) PAST: Paleontological statistic package for education and data analysis. Paleontol Electron 4, 9

Hickman GC (1985) Surface-mound formation by the tuco-tuco *Ctenomys fulvus* (Rodentia: Ctenomydae), with comments on earth-pushing in other fossorial mammals. J Zool 3:385-390

Hildebrand M (1974) Analysis of Vertebrate Structure. John Wiley & Sons Inc, New York

Hildebrand M (1985) Digging of Quadrupeds. Belknap Press of Harvard University Press, Cambridge

Hildebrand M, Goslow G (2001) Analysis of Vertebrate Structure. John Wiley & Sons Inc, New York

Holliger CD (1916) Anatomical Adaptations in the Thoracic Limb of the California Pocket Gopher and Other Rodents. University of California Press, Berkeley

Kardong KV (2002) Vertebrates: Comparative Anatomy, Function, Evolution (3rd ed). McGraw-Hill, Boston

Kielan-Jaworowska Z, Cifelli RL, Luo Z-X (2004) Mammals from the Age of Dinosaurs:Origins, Evolution, and Structure. Columbia University Press, New York

Kley NJ, Kearney M (2007) Adaptations for digging and burrowing. In: Hall B (ed) Fins into Limbs: Evolution, Development, and Transformation. University of Chicago Press, Chicago, pp 284-309

Landry SO (1958) The function of the entepicondylar foramen in mammals. Am Midl Nat 60:100-112

Larson SG (1993) Functional morphology of the shoulder in primates. In: Gebo DL(ed) Postcranial Adaptation in Nonhuman Primates. Northern Illinois University Press, DeKalb, pp 45-69

Lessa EP, Stein BR (1992) Morphological constraints in the digging apparatus of pocket gophers (Mammalia: Geomyidae). Biol J Linn Soc 47:439-453

Lessa EP, Thaeler CS Jr (1989) A reassessment of morphological specializations for digging in pocket gophers. J. Mammal 70:689-700

Loomis FB (1914) The Deseado Formation of Patagonia. Runford Press, Concord

Marshall LG, Swisher CC, Lavenu A, Hoffstetter R, Curtis GH (1992) Geochronology of the mammal-bearing late Cenozoic on the northern Altiplano, Bolivia. J South Am Earth Sci 5:1-19

Maynard Smith J, Savage RJG (1956) Some locomotory adaptations in mammals. Zool J Linn Soc 42:603-622

McEvoy JS (1982) Comparative myology of the pectoral and pelvic appendages of the North Amercian porcupine (*Erethizon dorsatum*) and the prehensile-tailed porcupine (*Coendou prehensilis*). Bull Am Mus Nat Hist 173:337-421

Meng J, Hu YM, Li CK (2003) The osteology of *Rhombomylus* (Mammalia, Glires): implications for phylogeny and evolution of glires. Bull Am Mus Nat Hist 275:1-247

Michener GR (2004) Hunting techniques and tool use by North American badgers preying on Richardson's ground squirrels. J Mammal 85: 1019-1027

Muizon C de (1998) *Mayulestes ferox*, a borhyaenoid (Metatheria, Mammalia) from the early Palaeocene of Bolivia. Phylogenetic and palaeobiological implications. Geodiversitas 20:19-142

Olson RA, Womble MD, Thomas DR, Glen ZD, Butcher MT (2015) Functional morphology of the forelimb of the nine-banded armadillo (*Dasypus novemcinctus*): comparative perspectives on the myology of Dasypodidae. J Mammal Evol 23:49-69

Patterson B (1975) The fossil aardvarks (Mammalia: Tubulidentata). Bull Mus Comp Zool 147:185-237

Paz ER, Kramarz A, Bond M (2011) Mesotheriid (Mammalia, Notoungulata) remains from the Colhuehuapian beds (early Miocene) of Chichinales Formation, Río Negro Province, Argentina. Ameghiniana 48:264-269

Polly PD (2007) Limbs in mammalian evolution. In: Hall BK (ed) Fins into Limbs: Evolution, Development, and Transformation. University of Chicago Press, Chicago, pp 245-268

Rose J, Moore A, Russell A, Butcher M (2014) Functional osteology of the forelimb digging apparatus of badgers. J Mammal 95:543-558

Rose MD (1993) Functional anatomy of the elbow and forearm in primates. In: Gebo DL (ed) Postcranial Adaptation in Nonhuman Primates. Northern Illinois University Press, Dekalb, pp 70–95

Rovereto C (1914) Los estratos araucanos y sus fósiles. Anales Mus Nac Hist Nat Buenos Aires 25: 1-250

Saint-André P-A (1993) *Hoffstetterius imperator* n. g., n. sp. du Miocène supérieur de l'Altiplano bolivien et le statut des Dinotoxodontinés (Mammalia, Notoungulata). C R Acad Sc 316:539-545

Salesa MJ, Anton M, Peigné S, Morales J (2008) Functional anatomy and biomechanics of the postcranial skeleton of *Simocyon batalleri* (Viret, 1929) (Carnivora, Ailuridae) from the late Miocene of Spain. Zool J Linn Soc 152:593-621

Sargis EJ (2002) Fucntional morphology of the forelimbs of tupaiids (Mammalia, Scandentia) and its phylogenetic implications. J Morphol 253:10-42

Schaller O (2007) Illustrated Veterinary Anatomical Nomenclature. Enke Verlag, Stuttgart

Serres M (1867) De l'ostéographie du *Mesotherium* et de ses affinities zoologiques. C R Acad Sci 65:140-148

Shockey BJ, Anaya F (2008) Postcranial osteology of mammals from Salla, Bolivia (late Oligocene): form, function, and phylogenetic implications In: Sargis EJ, Dagosto M (eds) Mammalian Evolutionary Morphology: A Tribute to Frederick S Szalay. Springer, Dordrecht, pp 135-157

Shockey BJ, Croft DA, Anaya F (2007) Analysis of function in the absence of extant functional homologues: a case study using mesotheriid notoungulates (Mammalia). Paleobiology 33:227-247

Shockey BJ, Flynn JJ, Croft DA, Gans PB, Wyss AR (2012) New leontiniid Notoungulata (Mammalia) from Chile and Argentina: comparative anatomy, character analysis, and phylogenetic hypotheses. Am Mus Novitates 3737:1-64

Stein BR (2000) Morphology of subterranean rodents. In: Lacey EA, Patton JL, Cameron G (eds) Life Underground: the Biology of Subterranean Rodents. University of Chicago Press, Chicago, pp 19-62

Szalay FS, Dagosto M (1980) Locomotor adaptations as reflected on the humerus of Paleogene primates. Folia Primatol 34:1– 45

Szalay FS, Sargis EJ (2001) Model-based analysis of postcranial osteology of marsupials from the Paleocene of Itaboraí, Brazil, and the phylogenetics and biogeography of Metatheria. Geodiversitas 23:139-302

Taylor BK (1978) The anatomy of the forelimb in the anteater (*Tamandua*) and its functional implications. J Morphol 157:347-368

Villarroel C (1974) Les mésothérinés (Notoungulata, Mammalia) du Pliocène de Bolivie et leurs rapports avec ceux d'Argentine. Ann Paléontol 60:245-281

Waibl H, Gasse H, Hashimoto Y (2005) Nomina Anatomica Veterinaria. International Committee on Veterinary Gross Anatomical Nomenclature, World Association of Veterinary Anatomists, Hannover